DOI: 10.1002/ejic.200900936

Synthesis and Photophysical Properties of Substituted Tris(phenylbenzimidazolinato) Ir^{III} Carbene Complexes as a Blue Phosphorescent Material

Kazuyoshi Tsuchiya,[a] Shiki Yagai,[a] Akihide Kitamura,[a] Takashi Karatsu,*[a] Kyoko Endo,[b] Junji Mizukami,[b] Seiji Akiyama,[b] and Masayoshi Yabe[b]

Keywords: Phosphorescence / Carbene ligands / OLEDs / Iridium / Density functional calculations

Substitution effects on the photoluminescence and electrochemical properties and the photochemical stability of tris(phenylbenzimidazolinato)Ir^{III} complexes were investigated. Facial and meridional isomers of a series of complexes having the general structure of Ir(C^C)$_3$, where (C^C) is (4-R-phenyl)benzimidazolinato (R = H, CF_3, CN, OCH_3), were prepared. They are abbreviated to Ir(pmb)$_3$ (**1**), Ir(CF_3pmb)$_3$ (**2**), Ir(CNpmb)$_3$ (**3**), and Ir(Opmb)$_3$ (**4**), respectively. Electron-donating or -withdrawing groups on the phenyl ring lead to both higher emission quantum yields and longer emission lifetimes compared to those of **1** in each *mer* and *fac* series. Particularly, the emission quantum yields were high in the cases of **2a**, **3a**, **3b**, and **4a**. No photochemical isomerization was observed in both *fac*- (a) and *mer* (b) isomers of Ir(pmb)$_3$, Ir(CF3pmb)$_3$, and Ir(CNpmb)$_3$ on irradiation with a 313-nm wavelength light from a 400 W mercury lamp for more than 20 h. All complexes excluding *fac*-Ir(pmb)$_3$ (**1a**) show excellent photochemical stability in degassed anhydrous thf solution. The locations of the HOMO and LUMO and the lowest excitation energy of these complexes were investigated by DFT and TD-DFT calculations on *fac*- and *mer*-Ir(Opmb)$_3$ (**4a** and **4b**). The HOMO is mainly localized over the Ir metal center and the phenyl moiety, and the LUMO mainly localized over the benzimidazole moiety. The calculated lowest excitation energies agree with the experimental values. The X-ray single crystal structures obtained for *fac*-Ir(CF_3pmb)$_3$ (**2a**) and *mer*-Ir(Opmb)$_3$ (**4b**) are also discussed.

Introduction

Iridium triscyclometalated complexes have recently caught significant attention because of their supreme phosphorescence performance for OLEDs (organic light-emitting diode).[1–5] For the fabrication of full color display, the colors red, green, and blue are required for the complexes, and their emission colors can be tuned by the structures of the ligands.[4–6] So far, pure and highly efficient phosphorescent green materials and relatively highly phosphorescent red materials have been achieved. The color red can be also obtained by using conjugated ancillary ligands.[7] Despite numerous attempts, it remains difficult to obtain the color blue. For the color blue, a high energy gap is required, therefore attempts to decrease the HOMO energy level[6–9] or increase the LUMO energy level were examined.[6,10] Tris(4,6-difluorophenylpyridinato)Ir [Ir(F_2ppy)$_3$] has a lower HOMO energy level than tris(phenylpyrazinato)Ir [Ir(ppy)$_3$] and presents a greenish-blue color.[6,8] Tris(phenylpyrazorinato)Ir [Ir(ppz)$_3$] has a higher LUMO energy level and emits a blue color in the solid state or at 77 K in glassy matrices, but no emission is observed in fluid solution at 298 K.[6,10] By using ancillary ligands such as pyridylpyrazolato, blue color emission at 298 K has been achieved, but this emission quantum yield remains low.[11] There are also some reports that discuss the reason why true blue color phosphorescent materials are not emissive at ambient temperature. It is theoretically suggested that the emissive state of Ir(ppz)$_3$ is high enough in energy to be thermally activated to the nonemissive d_π–d_{σ^*} state at ambient temperatures.[12] In 2005, Sajoto et al. reported phenylbenzimidazolinato and phenylimidazolinato Ir complexes with carbene ligands that exhibit near-UV phosphorescence with a relatively high quantum efficiency at room temperature.[13a] This is due to the strong ligand-field effect of the carbene ligand. As a result, the nonradiative d_π–d_{σ^*} state is kept largely away from the emissive triplet state, and therefore the complexes were actually used for OLEDs.[14] CN-substituted *fac*-Ir carbene complexes show smaller radiative rate constants than nonsubstituted complexes.[15] The luminescence properties and theoretical studies on Ir carbene complexes with ancillary ligands have also been reported,[16a] and recently, complexes having phosphane ligands show true blue phosphorescence with high external quan-

[a] Department of Applied Chemistry and Biotechnology, Graduate School of Engineering, Chiba University, 1-33, Yayoi-cho, Inage-ku, Chiba 263-8522, Japan
Fax: +81-43-290-3401
E-mail: karatsu@faculty.chiba-u.jp
[b] MCC-Group Science and Technology Reserch Center, Mitsubishi Chemical Corporation, 1000 Kamoshida, Aoba-ku, Yokohama 277-8522, Japan
Supporting information for this article is available on the WWW under http://dx.doi.org/10.1002/ejic.200900936.

WILEY InterScience DISCOVER SOMETHING GREAT
© 2010 Wiley-VCH Verlag GmbH & Co. KGaA, Weinheim

tum efficiencies for OLEDs.[16b] While many efforts to obtain highly efficient blue phosphorescent material were reported, the excited state properties of Ir carbene complexes remain unclear. The phosphorescence quantum yield of nonsubstituted *fac*-Ir(pmb)$_3$ has originally been reported to be 0.04;[13a] however, recently, this value was corrected to 0.37.[13b] Although, this value is smaller than that for *fac*-Ir(CNpmb)$_3$ (0.78).[15] In this paper, we investigate the substituent effects on the photophysics and photochemistry of Ir carbene complexes. In addition, we describe the simple one-step synthesis of Ir carbene complexes by reaction of $IrCl_3$ and a benzimidazolium iodide precursor. Phenylbenzimidazole with electron-withdrawing or electron-donating groups as substituents on the phenyl moieties was chosen as the ligand. Both *mer*- and *fac* isomers were prepared (Figure 1) to investigate their photochemical properties and geometrical isomerization. The single-crystal X-ray structures, photoluminescence properties, electrochemical properties, and photochemical stabilities of the complexes were investigated to explore the substitution effect on the Ir carbene complexes. DFT and TD-DFT calculations were also performed, and the calculated lowest excitation energy and the locations of the HOMO and LUMO were obtained.

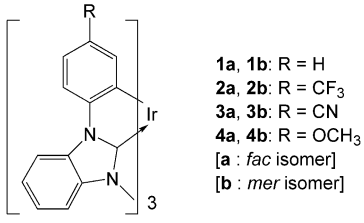

Figure 1. Chemical structures of Ir^{III} complexes studied.

Results and Discussion

Synthesis

The typical synthesis of triscyclometalated Ir^{III} complexes starts from the Ir^{III} μ-dichlorido-bridged dimer.[6,7a] The synthesis of Ir carbene complexes also uses such a method, from iridium trichloride hydrate and ligand iodide precursors (4.2 equiv.) in the presence of silver(I) oxide.[13a] The dimer complexes are then allowed to react with the ligand iodide precursors to give the final complexes. In the case of complex **1**, yields of the dimer and final complexes were reported to be 12.7 and 98%, respectively. Recently, the one-pot synthesis of Ir carbene complexes from [Ir(μ-Cl)(COD)$_2$]$_2$ (COD:cycloocta-1,5-diene) was reported.[17] [Ir(μ-Cl)(COD)$_2$]$_2$ and the ligand chloride precursors (6 equiv.) were treated in the presence of silver(I) oxide, and yields were between 58–79% depending on solvent used. In this work, the one-pot synthesis of Ir carbene complexes from $IrCl_3 \cdot 3H_2O$ by reaction with substituted phenylbenzimidazolium iodide precursors (3.2 equiv.) by using Ag_2CO_3 and Na_2CO_3 (Scheme 1) is reported. Use of these bases is one of the features of this method.

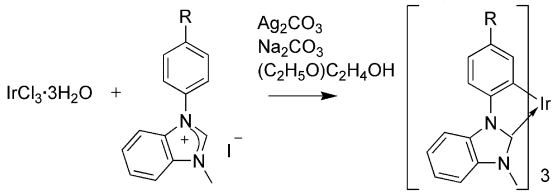

Scheme 1. Preparation of Ir triscyclometalated carbene complexes.

Substituted phenylbenzimidazolium iodide precursors were prepared according to the literature method.[13a,18] Ir^{III} triscyclometalated carbene complexes were prepared by heating a 2-ethoxyethanol solution of $IrCl_3 \cdot 3H_2O$ and the ligand iodide precursors at reflux in the presence of silver carbonate for 20 h; a mixture of *fac*- and *mer* isomers were obtained. These mixtures were separated by reprecipitation or by column chromatography and further purified by reprecipitation from CH_2Cl_2/CH_3OH to give pure complexes with yields ranging between 83% (in total for **2**, 62 and 21% for **2a** and **2b**, respectively) and 26.8% (in total for **3**, 5.8 and 21% for **3a** and **3b**, respectively) (for details see the Experimental Section).

Crystal Structure of Complex 2a and 4b

The single crystal of **2a** was obtained from a dichloroethane and ethanol solution by slow solvent evaporation,

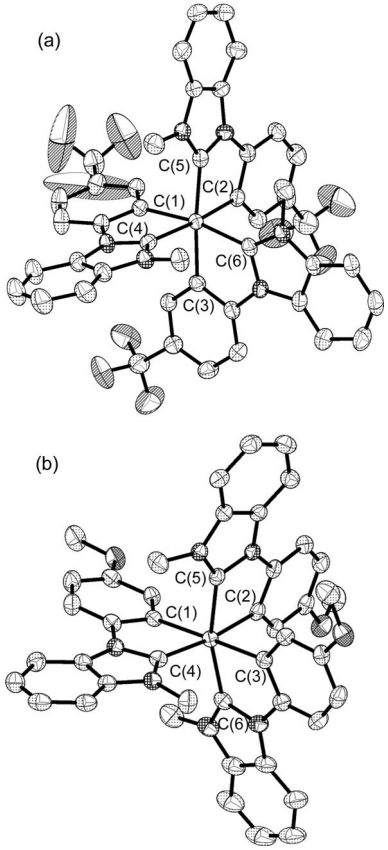

Figure 2. ORTEP diagram of (a) **2a** and (b) **4b**. The CF_3 groups of **2a** show large thermal anisotropy because of disorder; cocrystallized dichloroethane in (a) and the H atoms are omitted.

 © 2010 Wiley-VCH Verlag GmbH & Co. KGaA, Weinheim

and the single crystal of **4b** was obtained from CH_2Cl_2 and methanol. As depicted in Figure 2, complexes **2a** and **4b** show a distorted octahedral geometry. Selected bond lengths of **2a** and **4b** are listed in Table 1. In **2a**, the average bond lengths of the mutually *trans* Ir–C_{aryl} [2.081(4) Å] and Ir–$C_{carbene}$ bonds [2.033(4) Å] are almost identical to the average bond lengths of the Ir–C_{aryl} [2.081(7) Å] and Ir–$C_{carbene}$ bonds [2.026(7) Å] reported in **1a**.[13a] In **4b**, the bond lengths of the Ir–C_{aryl} bond *trans* to the benzimidazolyl group [Ir–C(2), 2.076(2) Å] and the Ir–$C_{carbene}$ bond *trans* to the phenyl group [Ir–C(4), 2.042(2) Å] are similar to those of **1b**, and the bond lengths of the mutually *trans* Ir–C_{aryl} [Ir–C(1), Ir–C(3) average 2.105(2) Å] and the Ir–$C_{carbene}$ bonds [Ir–C(5), Ir–C(6) average 2.020(2) Å] are almost same to those of **1b**[13a] [average mutually *trans* Ir–C_{aryl} 2.093(4) Å, average mutually *trans* Ir–$C_{carbene}$ 2.026(4) Å]. These indicate that the substituents on the phenyl moiety do not affect the core structure of complexes.

Table 1. Selected bond lengths in **2a** and **4b**.

	2a	**4b**
Ir–C(1)	2.079(4)	2.117(2)
Ir–C(2)	2.085(4)	2.076(2)
Ir–C(3)	2.078(4)	2.093(2)
Ir–C(4)	2.035(4)	2.042(2)
Ir–C(5)	2.033(4)	2.009(2)
Ir–C(6)	2.030(4)	2.030(3)

Photophysical Property

The UV/Vis absorption spectra and PL spectra of **1a**–**4b** are shown in Figure 3. The data are summarized in Table 2. The absorption band at lower energy (λ = 320–360 nm) can be ascribed to the ^{1}MLCT transition for all complexes.[2] By introducing substituents, the absorption and PL spectra of both the *mer*- and *fac* isomers were redshifted, regardless of the electron-withdrawing or -donating groups. The λ_{max} of the *mer* isomer appears at lower energy than those of the *fac* isomers, as for the reported triscyclometalated Ir complexes.[6,8,10] The magnitude of the redshift is in the order CN > OCH_3 > CF_3, and the redshift in the PL spectra is in the same order. This order of the redshift may originate from the π-conjugation ability of the substituents. The values for Φ_{PL} and τ for both isomer types for all the complexes are listed in Table 2. The rate constants are calculated by using the equations $k_r = \Phi_{PL}/\tau$ and $k_{nr} = (1 - \Phi_{PL})/\tau$. The k_r value for **3a** is almost the same as that obtained in the solid state.[14] The rate constant of *mer*-Ir(pmb)$_3$ is also similar to that of *mer*-Ir(ppy)$_3$. The k_r values for all the substituted complexes are smaller than those for **1a** and **1b** (unsubstituted complexes), and the difference between the *fac*- and *mer* isomers with the same substituent is small. The k_r value is not strongly affected by the structure of the geometrical isomers.

The Φ_{PL} and τ values for **1a** and **1b** were previously reported to be 0.04 and 0.22 μs and 0.002 and 0.015 μs, respectively;[13a] however, recently, those values for **1a** have been corrected to 0.37 and 1.1 μs. These values agree well with our data.

The increase in the k_{nr} values from the *fac* to the *mer* isomer differs for all the complexes. In the case of **3a** and **3b**, the k_{nr} value of **3a** is equivalent to that of **3b**; however, the k_{nr} value of the *mer* isomer is higher by one order of magnitude for **2b** and two orders of magnitude for **1b** and **4b**. As a result, when comparing the k_{nr} values with k_r in each complex, the Φ_{PL} values of **1b** and **4b** are very small. Substitution by the CF_3 and OMe groups lower the k_r value in both the *fac*- and *mer* isomers relative to those for com-

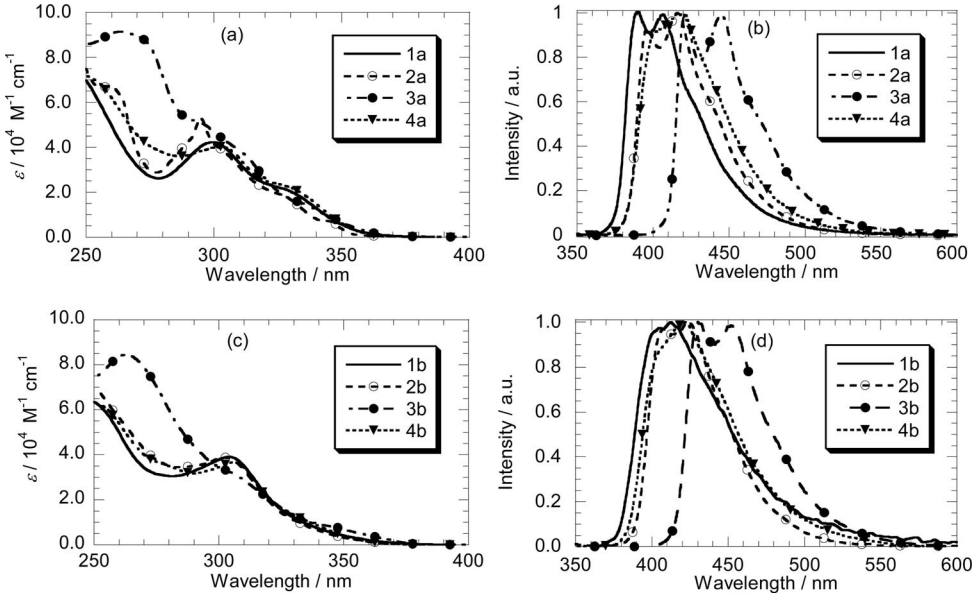

Figure 3. Absorption (a and c) and phosphorescence spectra (b and d) of **1**–**4** in anhydrous thf purged by argon.

 © 2010 Wiley-VCH Verlag GmbH & Co. KGaA, Weinheim

Table 2. Photoluminescent properties of Ir complexes **1a**–**4b** in degassed thf at 298 K.

Complex	λ_{em} [nm]	Φ_{PL}[a]	τ [μs]	$k_r/10^{-5}$ [s^{-1}]	$k_{nr}/10^{-5}$ [s^{-1}]
1a	390, 407	0.44[b]	1.3[b]	3.4	4.3
1b	405, 412	0.011[c]	0.024[c]	4.6	412
2a	396, 416	0.84	6.1	1.4	0.26
2b	407, 424	0.36	3.0	1.2	2.1
3a	421, 445	0.71[d]	14	0.51	0.21
3b	430, 452	0.63	15	0.42	0.25
4a	403, 415	0.76	5	1.5	0.48
4b	407, 422	0.054	0.26	2.1	36

[a] 9,10-Diphenylanthracene in cyclohexane (Φ = 0.90) was used as reference. [b] Φ_{PL} = 0.37 and τ = 1.1 μs in 2-Me(thf) was reported in ref.[13b] [c] Φ_{PL} = 0.002 and τ = 0.015 μs in 2-Me(thf) was reported in ref.[13a] [d] Φ_{PL} = 0.78 was reported for the sample doped in PMMA in ref.[15]

plex **1**, and substitution by the CN group largely lowers the k_r value in both the *fac*- and *mer* isomers. It appears that the k_r values are independent of the electron density of the phenyl moiety. The major nonradiative decay process of the blue phosphorescent complexes is believed to occur via the ligand-field excited state (i.e. d_π–d_σ* state).[13a] By substitution, the energetic separation between the LUMO and the d–d state is increased because of decrease in the LUMO energy level or because of the increase in the energy level of the d–d state; therefore the k_{nr} value decreases. Substitution by the CF_3 and CN groups leads to a large decrease in the k_{nr} value in the *mer* isomers relative to that in the unsubstituted complex **1**, and substitution by the OMe group leads to a decrease in the k_{nr} value in the *mer* isomer, but not as large as that observed for the cases of the CF_3 and CN groups. These results indicate that electron-withdrawing groups increase the energy separation between the phosphorescence state and the d–d state; however, electron-donating groups just slightly increase it. Complexes **3a** and **3b** show long lifetimes (14–15 μs). This is most likely because of the large separation between the ^{1}MLCT and ^{3}LC states (the difference in energy is ΔE_{ST}).[15,19] While the ^{1}MLCT energies estimated from the absorption spectra of **3a** and **3b** are almost same as those for the other complexes (c.a. 350 nm), the emission energies are lower than those for the others (c.a. 30 nm). This indicates that **3a** and **3b** have larger ΔE_{ST} values than those for the others; this is also supported by the time-resolved PL spectroscopy results at low temperature.[14] In the Ir(ppy)$_3$-based complexes, the fluorine or methyl substitution on the phenyl moiety affects neither the k_r nor the k_{nr} values.[6] Some heteroleptic Ir complexes such as Ir(pic)$_3$ or amide-bridged ppy and picolinato-based complexes show improvements in the quantum yield by substitution by the CF_3 group.[7d,20] In carbene complexes, similar substitution affects both the k_r and k_{nr} values; the effect is particularly large with substitution by the cyano group. The decrease in the k_{nr} value is because of the large separation between the d–d state and the ^{3}LC state, and the decrease in the k_r value is because of the increase in ΔE_{ST}.

Electrochemical Property

The oxidation potentials were determined by cyclic voltammetry in anhydrous thf and are summarized in Table 3. These results indicate that electron-withdrawing groups stabilize the HOMO energy and that the electron-donating groups destabilize the HOMO, and that the HOMO is spread largely over the phenyl moiety. We were not able to obtain the reduction potentials because the cyclic voltammograms are irreversible or do not appear in a scan area. From the UV/Vis absorption spectra, it is obvious that the ^{1}MLCT absorption bands appear in almost the same area for all complexes, while the oxidation potentials differ among the complexes. This indicates that in Ir carbene complexes, not only the HOMO but also the LUMO is largely affected by ligand substitution.

Table 3. Electrochemical property of the complexes.

Complex	$E_{1/2}^{OX}$[a]	
	a (*fac*)	**b** (*mer*)
1	0.45	0.42
2	0.74	0.59[b]
3	0.84[b]	0.84[b]
4	0.37[b]	0.29[c]

[a] Measured in anhydrous thf purged by argon, values are reported relative to Cp_2Fe/Cp_2Fe^+. [b] Voltammograms are not completely reversible. [c] Irreversible.

Photochemical Stability

It is known that some *mer* isomers of cyclometalated Ir complexes show photochemical *mer*→*fac* geometrical isomerization [*mer*-Ir(ppy)$_3$, *mer*-Ir(F$_2$ppy)$_3$, *mer*-Ir(tpy)$_3$, *mer*-Ir(ppz)$_3$],[6,8,10] and their reaction mechanisms have been discussed.[21] When Ir complexes are used as a phosphorescence dopant in OLEDs, high durability is needed, and one of the reasons for decomposition is chemical reaction in the excited state (it may be self-degradation or reaction with the host material surrounding the complexes). It is for this reason that we were motivated to examine the photochemical stabilities of the complexes. The Ir carbene complexes were dissolved in anhydrous thf, then degassed by freeze-pump-thaw cycles, and irradiated by 313 nm light from a 400 W, middle-pressure mercury lamp. In a previous study, *mer*-Ir(pmb)$_3$ and *mer*-Ir(pmi)$_3$ did not show photochemical geometrical isomerization,[13a] and it is assumed that substituted carbene complexes also do not show isomerization or have a very small isomerization quantum yield. To clarify this point, *mer*-Ir(tpy)$_3$, which has a quantum yield that is sufficiently small ($\Phi_{iso} = 1.8 \times 10^{-4}$), was used as a reference. The absorbance of the samples at the irradiation wavelength (Abs_{313}) was set between 1 and 3 (The concentration was between 3.6×10^{-5} and 1.5×10^{-4} M, and the volume of the solution was 3.5 mL). Figure S1 (Supporting Information) shows the change in the UV/Vis and PL spectra. When *mer*-Ir(tpy)$_3$ was irradiated for 3 h, only 3.0×10^{-8} mol of the complex isomerized. In **1a**, although slight decrease in the absorption spectra was observed, 30%

 © 2010 Wiley-VCH Verlag GmbH & Co. KGaA, Weinheim

of the photoluminescence intensity was quenched after irradiation for 45 h. At this point, no *mer* isomer was observed by HPLC. TLC analysis indicates that a spot appeared by development in a hexane/ethyl acetate (7:3) mixture. However, we failed to identify the product. Other complexes (**2a**, **2b**, **3a**, and **3b**) showed photoirradiation robustness upon irradiation for 20–45 h. From the results of the *mer*- or even the *fac* isomers, we conclude that not only **1a** and **1b** but also **2a**, **2b**, **3a**, and **3b** do not undergo geometrical isomerization. The first step in the photochemical isomerization of cyclometalated Ir complexes such as *mer*-Ir(ppz)$_3$ and *mer*-Ir(tpy)$_3$ is bond rapture from the d_π–d_σ* state,[12] followed by hybridization to the trigonal-bipyramidal structure, and finally, rehybridization to the octahedral structure completes the isomerization. In the case of carbene-type iridium complexes, it is thought that thermal activation to the d_π–d_σ* state in the excited state also occurs because the k_{nr} value of **1b** is large. There are two reasons why **1b** does not show photochemical isomerization; bond rapture from the d_π–d_σ* state may not occur or the activation energy barrier for isomerization is too large. The other carbene complexes **2b**–**4b** also do not show photochemical isomerization. In **2b** and **3b**, the k_{nr} values are small, therefore, thermal activation to the d_π–d_σ* state in the excited state may not occur. Recently, deactivation of blue phosphorescent *fac* complexes have been reported.[22] The temperature dependence of the phosphorescence indicates thermal activation to the nonradiative decay state. A similar state of the *mer* isomer is also proposed as a key state for the *mer*→*fac* geometrical isomerization;[8,10,21] however, the *mer* isomers of the carbene complexes did not isomerize to the corresponding *fac* isomer. This may indicate that a high activation energy is needed to access the key state for the *mer* isomer of the carbene complexes. In total, the photochemical stability of **1b**, **2a**, **2b**, **3a**, **3b**, **4a**, and **4b** is very high in degassed solution.

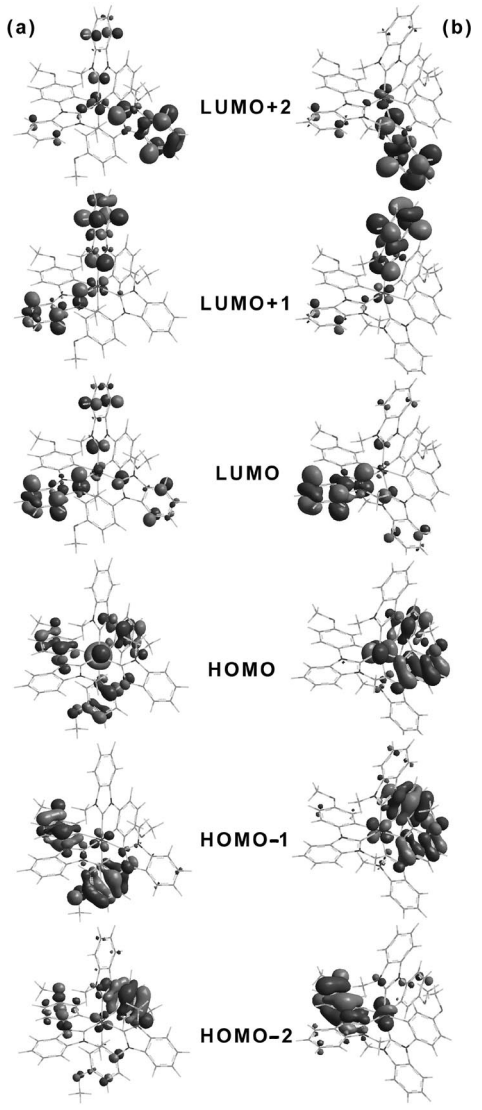

Figure 4. Frontier orbitals of *fac*- (a; left column) and *mer*-Ir(Opmb)$_3$ (b; right column) (**4a** and **4b**) obtained for the optimized structures of the ground state.

DFT and TD-DFT Calculation

The location of the molecular orbital was calculated by using the optimized geometry of the ground state. It is revealed that in both **4a** and **4b**, the HOMO–2 to HOMO are delocalized over the Ir-phenyl moiety, and the LUMO to LUMO+2 are delocalized over the benzimidazole moiety (Figure 4). These results are similar to those for Ir(ppz)$_3$. As was established by cyclic voltammetry, substitution on the phenyl moiety affects the HOMO level; however, we could not comment on the LUMO level because it was difficult to observe the reduction potentials. However, as the HOMO level is stabilized by electron-withdrawing groups, the excitation energy also decreases.

This indicates that the LUMO level also decreases. By MO consideration, although the LUMO is mainly spread over the benzimidazole moiety, the substituents on the phenyl moiety affect both the HOMO and LUMO energies.

We then performed TD-DFT calculations. TD-DFT is a useful tool for understanding Ir complexes, as shown in the literature recently.[7e,16,23] The calculated lowest-excitation wavelength of **4a** and **4b** are 393.1 and 388.9 nm for the S_0–T_1 absorption, respectively, and 361.0 and 371.9 nm for the S_0–S_1 absorption, respectively. The results for the S_0–T_1 absorption wavelength agree with those determined experimentally by emission spectroscopy. In **4a**, the main transition for the S_0–T_1 absorption is HOMO→LUMO+2 (51%), which corresponds to the Ir-phenyl→benzimidazole transition. In **4b**, the main transition for the S_0–T_1 absorption is HOMO→LUMO (58.9%), which corresponds to the Ir-phenyl→equatorial benzimidazole transition. These results suggest that substitution does not affect the energy level of the LUMO, but it is also thought that an increase in ΔE_{ST} takes place. This question is still under investigation (Table 4 and Table 5).

 © 2010 Wiley-VCH Verlag GmbH & Co. KGaA, Weinheim

Table 4. Calculated transition wavelength, oscillator strength (*f*), and MOs involved in the lowest-energy transition of **4a** and **4b**.

Complex	State	λ_{max} [nm]	*f*	Assignments
4a	T_1	393.1	0	HOMO→LUMO+2 (51%)
				HOMO–2→LUMO+1 (11.9%)
				HOMO→LUMO+1 (10.6%)
	S_1	361.0	0.0509	HOMO→LUMO+1 (69.0%)
				HOMO→LUMO+2 (31.1%)
4b	T_1	388.9	0	HOMO→LUMO (58.8%)
				HOMO→LUMO+1 (16.8%)
				HOMO→LUMO+2 (11.5%)
	S_1	371.91	0.0062	HOMO→LUMO (95.6%)

Table 5. Calculated transition wavelength, oscillator strength (*f*), and MOs involved in the transitions of **4a** and **4b**.

Complex	State	λ_{max} [nm]	*f*	Assignments
4a	T_1	393.1	0	HOMO→LUMO+2 (51%)
	T_2	391.5	0	HOMO→LUMO+1 (30.1%)
	T_3	390.4	0	HOMO→LUMO (50.7%)
	S_1	361.0	0.0509	HOMO→LUMO+1 (69.0%)
	S_2	357.2		HOMO→LUMO+2 (68.4%)
4b	T_1	388.9	0	HOMO–2→LUMO (53.9%)
	T_2	381.85	0	HOMO→LUMO+1 (31.4%)
	T_3	374.2	0	HOMO→LUMO+2 (11.5%)
	S_1	371.91	0.0062	HOMO→LUMO (95.6%)
	S_2	359.6	0.0112	HOMO→LUMO+1 (95.3%)

Conclusions

Substituted tris(phenylbenzimidazolinato) Ir^{III} carbene complexes were prepared by a one-pot synthesis, and their structures, photophysical properties, electrochemical properties, and photochemical stabilities were investigated. The location of the HOMO and LUMO and lowest-excitation energy were calculated by TD-DFT. The structures are not affected by both electron-withdrawing and electron-donating groups. From cyclic voltammetry, the oxidative potential energy is stabilized by electron-withdrawing groups and slightly destabilized by electron-donating groups. The luminescent properties are affected greatly by the functional group on the phenyl moiety. The difference in the k_r values between the *fac*- and *mer* isomers having the same functional group is small but the difference in the k_{nr} values between the *fac*- and *mer* isomers is large for $Ir(pmb)_3$ and $Ir(Opmb)_3$, relatively small for $Ir(CF_3pmb)_3$, and very small for $Ir(CNpmb)_3$. From the DFT calculations, the HOMO is delocalized over the Ir-phenyl moiety, and LUMO, LUMO+1, and LUMO+2 are delocalized over the benzimidazole moiety. The calculated lowest triplet excited energies show good agreement with experimental data. We are currently evaluating the electroluminescence performance of OLEDs fabricated from the above complexes.

Experimental Section

General Information and Material: All chemicals used for the synthesis were purchased from Aldrich, Kanto Chemical, TCI, Wako Pure Chemical Industries, Kishida Chemical, N. E. Chemcat, and Fluya Metal and used without further purification. Ir carbene complexes were prepared by the one-pot synthesis method reported in the literature with minimal modification.[13a] Silver carbonate was used instead of silver oxide when $IrCl_3$ and the iodide ligand were treated (Scheme 1). Both the *fac*- and *mer* isomers were formed by reflux in 2-ethoxyethanol. The yield varied depending on the type of ligand. All complexes were prepared by the same procedure. ^1H NMR and ^{13}C NMR spectra were recorded on JEOL JNM-LA 400 and Bruker AVANCE 300 instruments. FAB mass spectra were recorded on a JEOL JMS-AX500 double focusing mass spectrometer, and EM-SI mass spectra were recorded on a Thermo Scientific Exactive mass spectrometer. Elemental analysis was performed with a Parkin-Elmer 2400 instrument.

Synthesis of *fac*-$Ir(CF_3pmb)_3$ and *mer*-$Ir(CF_3pmb)_3$ (Example): 1-methyl-3-(4-trifluoromethylphenyl)benzimidazolium iodide (2.1 g, 5.2 mmol), $IrCl_3{\cdot}3H_2O$ (0.58 g, 1.65 mmol), silver carbonate (0.71 g, 2.6 mmol), sodium carbonate (0.28 g, 2.6 mmol), and ethoxyethanol(50 mL) were heated at reflux for 20 h. Both the *mer*- and *fac* isomers were formed. After the mixture was cooled to room temperature and diluted with water, and the resultant precipitate was filtered off and washed with water and methanol, the crude product was purified by silica gel column chromatography. The *mer*- and *fac* isomers were successfully separated. On reprecipitation from a CH_2Cl_2 and CH_3OH mixture, the desirable compound was obtained as a white solid. Yield: *fac*-$Ir(CF_3pmb)_3$ (1.1 g, 68%), *mer*-$Ir(CF_3pmb)_3$ (0.38 g, 23%) (yield with respect to $IrCl_3{\cdot}3H_2O$).

***fac*-Iridium(III) Tris[1-(4-trifluoromethylphenyl)-3-methylbenzimidazolin-2-ylidene] (2a):** Yield: 1.1 g (68% with respect to $IrCl_3{\cdot}3H_2O$). ^1H NMR (400 MHz, $CDCl_3$): δ = 8.14 (d, J = 7.9 Hz, 3 H, $bzim^7$), 7.90 (d, J = 8.3 Hz, 3 H, $bzim^4$), 7.36 (ddd, J = 7.9, 7.5, 1.2 Hz, 3 H, $bzim^6$), 7.33 (dd, J = 8.3, 2.0 Hz, 3 H, Ph^5), 7.29 (ddd, J = 8.3, 7.5, 0.8 Hz, 3 H, $bzim^5$), 7.22 (dd, J = 8.3, 0.79 Hz, 3 H, Ph^6), 6.74 (d, J = 2.0 Hz, 3 H, Ph^3), 3.27 (s, 9 H, N-CH_3) ppm. ^{13}C NMR (100 MHz, dmso): δ = 187.07 (3 C, $bzim^2$), 151.35 (3 C, Ph^1), 148.60 (3 C, Ph^2), 135.75, 131.53, 131.27, 126.04, 124.43, 124.13, 123.57, 123.31, 122.87, 119.01, 111.96, 111.38, 111.18 (33C, $Ph^{3,4,5,6}$, $bzim^{3a,4,5,6,7,7a}$, CF_3) 33.22 (3 C, N-CH_3) ppm. HRMS(EM-SI): calcd. for $C_{45}H_{31}F_9IrN_6$ $[M + H]^+$ 1019.2090; found 1019.2094. $C_{45}H_{30}F_9IrN_6$ (1017.96): calcd. C 53.09, H 2.97, N 8.26; found C 52.68, H 2.40, N 8.08.

***mer*-Iridium(III) Tris[1-(4-trifluoromethylphenyl)-3-methylbenzimidazolin-2-ylidene] (2b):** Yield: 0.38 g (23% with respect to $IrCl_3{\cdot}3H_2O$). ^1H NMR (400 MHz, $CDCl_3$): δ = 8.16 (d, J = 8.3 Hz, 1 H, $bzim^7$), 8.15 (d, J = 7.9 Hz, 1 H, $bzim^7$), 8.11 (d, J = 7.9 Hz, 1 H, $bzim^7$), 7.90 (d, J = 8.2 Hz, 1 H, $bzim^4$), 7.89 (d, J = 8.0 Hz, 1 H, $bzim^4$), 7.88 (d, J = 8.9 Hz, 1 H, $bzim^4$), 7.43–7.23 (m, 12 H, $bzim^{5,6}$, $Ph^{5,6}$), 7.06 (d, J = 2.0 Hz, 1 H, Ph^3), 6.95 (d, J = 2.0 Hz, 1 H, Ph^3), 6.76 (d, J = 2.0 Hz, 1 H, Ph^3), 3.27 (s, 3 H, N-CH_3), 3.24 (s, 3 H, N-CH_3), 3.17 (s, 3 H, N-CH_3) ppm. ^{13}C NMR (100 MHz, $CDCl_3$): δ = 186.76, 185.07, 183.85 (3 C, $bzim^2$), 152.08, 151.52, 150.46 (3 C, Ph^1), 149.58, 148.80, 147.62 (3 C, Ph^2), 136.60, 136.55, 136.11, 134.72, 132.60, 132.31, 126.38, 126.26, 126.08, 125.95, 123.55, 123.51, 123.43, 123.35, 122.85, 122.58, 118.95, 118.85, 118.62, 112.18, 111.96, 111.85, 111.49, 111.33, 110.17, 110.07, 109.94 (33 C, $Ph^{3,4,5,6}$, $bzim^{3a,4,5,6,7,7a}$, CF_3), 33.63, 33.50, 32.78 (N-CH_3) ppm. HRMS (EM-SI): calcd. for $C_{45}H_{31}F_9IrN_6$ $[M + H]^+$ 1019.2094; found 1019.2094. $C_{45}H_{30}F_9IrN_6$ (1017.96): calcd. C 53.09, H 2.97, N 8.26; found C 52.82, H 2.63, N 7.85.

***fac*-Iridium(III) Tris(4-cyanophenyl-3-methylbenzimidazolin-2-ylidene) (3a):** Yield: 0.084 g (5.8% with respect to $IrCl_3{\cdot}3H_2O$). ^1H NMR (400 MHz, CD_2Cl_2): δ = 8.14 [d, J = 8.2 Hz, 3 H, ($bzim^7$)], 7.94 (d, J = 8.2 Hz, 3 H, $bzim^4$), 7.40 (dd, J = 8.2, 1.9 Hz, 3 H,

 © 2010 Wiley-VCH Verlag GmbH & Co. KGaA, Weinheim

Ph[5]), 7.39 (ddd, J = 8.2, 7.6, 1.8 Hz, 3 H, bzim[6]), 7.32 (ddd, J = 8.2, 7.5, 1.0 Hz, 3 H, bzim[5]), 7.28 (dd, J = 8.2, 1.0 Hz, 3 H, Ph[6]), 6.73 (d, J = 1.8 Hz, 3 H, Ph[3]), 3.25 (s, 9 H, N-CH_3) ppm. MS (FAB): calcd. 889.23; found 889. $C_{45}H_{30}IrN_9$ (889.00): calcd. C 60.80, H 3.40, N 14.18; found C 60.41, H 3.03, N 14.07.

***mer*-Iridium(III) Tris(4-cyanophenyl-3-methylbenzimidazolin-2-ylidene) (3b):** Yield: 0.31 g (21% with respect to $IrCl_3{\cdot}3H_2O$). ^{1}H NMR (400 MHz, $CDCl_3$): δ = 8.14 (d, J = 8.3 Hz, 3 H, bzim[7]), 7.91 (d, J = 8.2 Hz, 2 H, bzim[4]), 7.89 (d, J = 8.1 Hz, 1 H, bzim[4]), 7.48–7.24 (m, 12 H, Ph[5,6], bzim[5,6]), 7.06 (d, J = 1.8 Hz, 1 H, Ph[3]), 7.04 (d, J = 1.9 Hz, 1 H, Ph[3]), 6.76 (d, J = 1.8 Hz, 1 H, Ph[3]), 3.28 (s, 3 H, N-CH_3), 3.20 (s, 3 H, N-CH_3), 3.17 (s, 3 H, N-CH_3) ppm. ^{13}C NMR (100 MHz, $CDCl_3$): δ = 186.27, 184.84, 183.15 (3 C, bzim[2]), 152.74, 152.07, 151.18 (3 C, Ph[1]), 149.45, 149.01, 147.04 (3 C, Ph[2]), 141.51, 141.48, 139.41, 136.49, 136.46, 136.05, 132.07, 126.95, 126.68, 126.40, 124.03, 123.95, 123.92, 123.47, 123.39, 123.21, 120.59, 120.35, 112.65, 112.35, 111.88, 111.62, 111.44, 110.63, 110.41, 110.36, 108.10, 107.88, 107.74 (33 C, Ph[3,4,5,6], bzim[3a,4,5,6,7,7a], CN), 33.86, 33.82, 32.95 (3 C, N-CH_3) ppm. HRMS (EM-SI): calcd. for $C_{45}H_{30}IrN_9$ $[M + H]^+$ 890.23; found 890.23. $C_{45}H_{30}IrN_9{\cdot}0.5H_2O$ (898.01): calcd. C 60.17, H 3.48, N 14.04; found C 60.02, H 3.23, N 13.73.

***fac*-Iridium(III) Tris[1-(4-methoxyphenyl)-3-methylbenzimidazolin-2-ylidene] (4a):** Yield: 0.67 g (45% with respect to $IrCl_3{\cdot}3H_2O$). ^{1}H NMR (400 MHz, $CDCl_3$): δ = 8.07 (d, J = 8.2 Hz, 3 H, bzim[7]), 7.74 (d, J = 8.6 Hz, 3 H, bzim[4]), 7.28 (ddd, J = 8.2, 6.4, 1.5 Hz, 3 H, bzim[6]), 7.20 (ddd, J = 8.6, 6.4, 0.89 Hz, 3 H, bzim[5]), 7.16 (dd, J = 8.1, 1.3, Hz, 3 H, Ph[6]), 6.56 (dd, J = 8.6, 2.9 Hz, 3 H, Ph[5]), 6.26 (d, J = 3.0 Hz, 3 H, Ph[3]), 3.50 (s, 9 H, OCH_3), 3.24 (s, 9 H, N-CH_3) ppm. MS (FAB): calcd. 904.27; found 905. $C_{45}H_{39}IrN_6O_3$ (904.05): calcd. C 59.78, H 4.35, N 9.30; found C 59.51, H 4.06, N 9.24.

***mer*-Iridium(III) Tris[1-(4-methoxyphenyl)-3-methylbenzimidazolin-2-ylidene](4b):** Yield: 0.19 g (13% with respect to $IrCl_3{\cdot}3H_2O$). ^{1}H NMR (400 MHz, $CDCl_3$): δ = 8.11 (d, J = 8.2 Hz, 1 H, bzim[7]), 8.09 (d, J = 8.1 Hz, 1 H, bzim[7]), 8.03 (d, J = 8.1 Hz, 1 H, bzim[7]), 7.75 (d, J = 8.5 Hz, 1 H, bzim[4]), 7.74 (d, J = 8.5 Hz, 1 H, bzim[4]), 7.71 (d, J = 8.5 Hz, 1 H, bzim[4]), 7.35–7.16 (m, 9 H, bzim[6,7], Ph[6]), 6.56 (m, 5 H, Ph[3,5]), 6.20 (d, J = 2.9 Hz, 1 H, Ph[3]), 3.55 (s, 3 H, OCH_3), 3.54 (s, 3 H, OCH_3), 3.52 (s, 3 H, OCH_3), 3.30 (s, 3 H, N-CH_3), 3.22 (s, 3 H, N-CH_3), 3.21 (s, 3 H, N-CH_3) ppm. MS (FAB): calcd. 904.27; found 905. $C_{45}H_{39}IrN_6O_3$ (904.05): calcd. C 59.78, H 4.35, N 9.30; found C 59.45, H 4.05, N 9.13.

***fac*-Iridium(III) Tris(1-phenyl-3-methylbenzimidazolin-2-ylidene) (1a):** Yield: 0.35 g (26% with respect to $IrCl_3{\cdot}3H_2O$): ^{1}H NMR (400 MHz, $CDCl_3$): δ = 8.14 (d, J = 8.2 Hz, 3 H, bzim[7]), 7.86 (d, J = 7.4 Hz, 3 H, bzim[4]), 7.29 (td, J = 7.7, 1.4 Hz, 3 H, bzim[6]), 7.22 (t, J = 6.5 Hz, 3 H, bzim[5]), 7.17 (dd, J = 7.9, 0.95 Hz, 3 H, Ph[6]), 7.06 (td, J = 7.6, 1.5 Hz, 3 H, Ph[5]), 6.73 (td, J = 7.3, 0.73 Hz, 3 H, Ph[4]), 6.68 (dd, J = 7.2, 1.4 Hz, 3 H, Ph[3]), 3.27 (s, 9 H, N-CH_3) ppm. ^{13}C NMR (100 MHz, $CDCl_3$: δ = 189.64 (3 C, bzim[2]), 148.76, 148.65, (6 C, Ph[1,2]) 137.03, 136.35, 132.68, 124.67, 122.63, 121.69, 120.88, 112.01, 111.18, 109.52 (30 C, Ph[3,4,5,6], bzim[3a,4,5,6,7,7a]), 33.45 (3 C, N-CH_3). MS (FAB): calcd. 814.24; found 814.

***mer*-Iridium(III) Tris(1-phenyl-3-methylbenzimidazolin-2-ylidene) (1b):** Yield: 0.17 g (13% with respect to $IrCl_3{\cdot}3H_2O$). ^{1}H NMR (400 MHz, $CDCl_3$): δ = 8.18 (d, J = 8.2 Hz, 1 H, bzim[7]), 8.16 (d, J = 8.2 Hz, 1 H, bzim[7]), 8.10 (d, J = 8.2 Hz, 1 H, bzim[7]), 7.85 (d, J = 7.2 Hz, 1 H, bzim[4]), 7.83 (d, J = 7.5 Hz, 1 H, bzim[4]), 7.81 (d, J = 6.7 Hz, 1 H, bzim[4]), 7.38–7.18 (m, 9 H, Ph[6], bzim[5,6]), 7.05–6.97 (m, 2 H, Ph[5]), 6.94 (td, J = 7.6, 1.5 Hz, 1 H, Ph[5]), 6.90 (dd, J = 7.24, 1.6 Hz, 1 H, Ph[4]), 6.85 (dd, J = 7.2, 1.4 Hz, 1 H, Ph[4]), 6.71 (td, J = 7.3, 0.94 Hz, 1 H, Ph[4]), 6.67 (td, J = 7.2, 0.94 Hz, 1 H, Ph[3]), 6.64–6.58 (m, 2 H, Ph[3]), 3.28 (s, 3 H), 3.25 (s, 3 H), 3.19 (s, 3 H) ppm. ^{13}C NMR (100 MHz, $CDCl_3$): δ = 188.40, 186.15, 185.03 (3 C, bzim[2]), 150.87, 149.72, 149.35, 148.90, 147.96, 147.92 (6 C, Ph[1,2]), 144.13, 139.20, 139.03, 136.76, 136.71, 136.35, 132.67, 132.61, 132.59, 124.85, 124.62, 124.43, 122.68, 122.51, 121.91, 121.82, 121.52, 120.65, 120.32, 120.28, 112.45, 111.83, 111.24, 111.15, 109.70, 109.60, 109.46 (30 C, Ph[3,4,5,6], bzim[3a,4,5,6,7,7a]), 33.42, 33.35, 32.81 (3 C, N-CH_3) ppm. MS (FAB): calcd. 814.24; found 814.

X-ray Crystallography: The single crystal of *fac*-$Ir(CF_3pmb)_3$ was grown from $C_2H_2Cl_2/CH_3OH$ and that of *mer*-$Ir(Opmb)_3$ was grown from CH_2Cl_2/CH_3OH. Diffraction data were collected on a Bruker SMART APEX II CCD diffractometer at 173 K with graphite monochromated Mo-Ka radiation. Initial atomic positions were located by Patterson methods for **2a** and direct methods for **4b**. The structures were refined by least-squares method with the program XShell. CCDC-746571 and -746572 contain the supplementary crystallographic data for **2a** and **4b**, respectively. These data can be obtained free of charge from The Cambridge Crystallographic Data Centre via www.ccdc.cam.ac.uk/data_request/cif.

Electrochemistry: Cyclic voltammetry was performed with a standard compartment cell equipped with a BAS Pt working electrode, a platinum wire counter electrode, and a Ag/Ag^+ ($Ag/AgNO_3$) reference electrode with a HOKUTO DENKO HABF1510m analyzer. Anhydrous thf was used as a solvent, and tetrabutylammonium tetrafluoroborate was used as a supporting electrolyte. All potentials were reported relative to Cp_2Fe/Cp_2Fe^+.

DFT and TD-DFT Calculations: DFT and TD-DFT calculations were performed with the Gaussian 03 package[24] at the B3LYP/LANL2DZ level; 6-31G basis sets were employed. The structures obtained from X-ray crystallography were optimized, and the location of molecular orbitals such as HOMO and LUMO were calculated with the ground state. TD-DFT calculations were performed with the ground-state geometry to obtain the vertical excitation energies of the low-lying singlet and triplet excited states of the complexes.

Photophysical Properties: UV/Vis absorption spectra were measured on a JASCO-U570 spectrophotometer. PL spectra were measured on a JASCO F6010 fluorimeter. The response of the instrument was corrected by using rhodamine B standard solution. Sample thf solutions were degassed in the side-necked reservoir by performing the freeze-pump-thaw cycles three times and introduced into a 1-cm path length cuvette. Phosphorescence quantum yields were determined by using 9,10-diphenylanthracene in cyclohexane (Φ = 0.90) as reference, and the formula $\Phi_X = \Phi_S \times (n_X/n_S)^2 \times (A_X/A_S) \times (Abs_S/Abs_X)$ was used. The subscripts X and S indicate the sample and the reference, respectively, and n is the reflective index of the solvent, A is the area of the emission spectra, and Abs is the absorbance at the excitation wavelength (Abs is set around 0.20). The PL lifetimes were measured by a single photon counting instrument (Horiba NAES 550) or by a SPEX 270 M spectrometer equipped with a photomultiplier tube and a Hewlett Packard 54510B digital oscilloscope by using a Hoya Continuum Surelite-I Nd^{3+}:YAG laser with a 355-nm pulse as excitation source. Stabilizer-free anhydrous thf was used as the solvent for measuring the PL quantum yields and PL lifetimes (purchased from Wako Chemicals).

Photochemical Stability: The photochemical stability was examined in anhydrous thf solution degassed by performing the freeze-pump-thaw cycles three times. A 313-nm light from a 400-W middle-pressure mercury lamp (RIKO) was used to irradiate the samples. *fac*-

 © 2010 Wiley-VCH Verlag GmbH & Co. KGaA, Weinheim

$Ir(tpy)_3$ was used as a reference for determining the photochemical isomerization quantum yield. The reaction was monitored by UV/Vis and PL spectroscopy . After 20–40 h of irradiation, the sample tube was opened, and the sample was condensed by evaporation of the solvent and analyzed by TLC.

Supporting Information (see footnote on the first page of this article): UV and PL spectra of the complexes (**1a**–**4b**) before and after irradiation are presented.

Acknowledgments

The authors thank Prof. Motohiro Akazome (Chiba University) and Prof. Katsumi Tokumaru (University of Tsukuba) for helpful discussions. The authors thank the Analytical Center of Chiba University for helping with analysis of the materials. This work was supported by Grants-in-Aids for Scientific Research from the Ministry of Education, Culture, Sports, Science and Technology (MEXT) (No. 20550056).

[1] a) M. A. Baldo, D. F. O'Brien, Y. You, A. Shoustikov, S. Sibley, M. E. Thompson, S. R. Forrest, *Nature* **1998**, *395*, 151–154; b) M. A. Baldo, S. Lamansky, P. E. Burrows, M. E. Thompson, S. R. Forrest, *Appl. Phys. Lett.* **1999**, *75*, 4–6.

[2] H. Yersin (Ed.), *Highly Efficient OLEDs with Phosphorescent Materials*, Wiley-VCH, Weinheim, **2008** references cited therein.

[3] Y.-L. Tung, S.-W. Lee, Y. Chi, Y.-T. Tao, C.-H. Chien, Y.-M. Cheng, P.-T. Chou, S.-M. Peng, C.-S. Liu, *J. Mater. Chem.* **2005**, *15*, 460–464.

[4] a) A. Tsuboyama, H. Iwawaki, M. Furugori, T. Mukaide, J. Kamatani, S. Igawa, T. Moriyama, S. Miura, T. Takiguchi, S. Okada, M. Hoshino, K. Ueno, *J. Am. Chem. Soc.* **2003**, *125*, 12971–12979; b) M. Tavasli, S. Bettington, I. F. Perepichka, A. S. Batsanov, M. R. Bryce, C. Rothe, A. P. Monkman, *Eur. J. Inorg. Chem.* **2007**, 4808–4814.

[5] S. Tokito, T. Iijima, T. Tsuzuki, F. Sato, *Appl. Phys. Lett.* **2003**, *83*, 2459–2461.

[6] A. Tamayo, B. D. Alleyne, P. I. Djurovich, S. Lamansky, I. Tsyba, N. N. Ho, R. Bau, M. E. Thompson, *J. Am. Chem. Soc.* **2003**, *125*, 7377–7387.

[7] a) S. Lamansky, P. Djurovich, D. Murphy, F. A.-Razzaq, H.-E. Lee, C. Adachi, P. E. Burrows, S. R. Foorest, M. E. Thompson, *J. Am. Chem. Soc.* **2001**, *123*, 4304–4312; b) Y. You, S. Y. Park, *J. Am. Chem. Soc.* **2005**, *127*, 12438–12439; c) S. Kappaun, S. Eder, S. Sax, K. Mereiter, E. J. W. List, C. Slugove, *Eur. J. Inorg. Chem.* **2007**, 4207–4215; d) C. Yi, C.-J. Yang, J. Liu, M. Xu, J.-H. Wang, Q.-Y. Cao, X.-C. Gao, *Inorg. Chim. Acta* **2007**, *360*, 3493–3498; e) X. Gu, T. Fei, H. Zhang, H. Xu, B. Yang, Y. Ma, X. Liu, *Eur. J. Inorg. Chem.* **2009**, 2407–2414.

[8] T. Karatsu, T. Nakamura, S. Yagai, A. Kitamura, K. Yamaguchi, Y. Matsushima, T. Iwata, Y. Hori, T. Hagiwara, *Chem. Lett.* **2003**, *32*, 886–887.

[9] a) M. Xu, R. Zhou, G. Wang, Q. Xiao, W. Du, G. Che, *Inorg. Chim. Acta* **2008**, *361*, 2407–2412; b) H. Jang, C. H. Shin, N. G. Kim, K. Y. Hwang, Y. Do, *Synth. Met.* **2005**, *154*, 157–160.

[10] T. Karatsu, E. Ito, S. Yagai, A. Kitamura, *Chem. Phys. Lett.* **2006**, *424*, 353–357.

[11] C.-H. Yang, S.-W. Li, Y. Chi, Y.-M. Cheng, Y.-S. Yeh, P.-T. Chou, G.-H. Lee, C.-H. Wang, C.-F. Shu, *Inorg. Chem.* **2005**, *44*, 7770–7780.

[12] a) G. Treboux, J. Mizukami, M. Yabe, S. Nakamura, *Chem. Lett.* **2007**, *36*, 1344–1345; b) L. Yang, F. Okada, K. Kobayashi, K. Nozaki, Y. Tanabe, Y. Ishii, M. Haga, *Inorg. Chem.* **2008**, *47*, 7154–7165.

[13] a) T. Sajoto, P. I. Djurovich, A. B. Tamayo, M. Yousufuddin, R. Bau, M. E. Thompson, R. J. Holmes, S. R. Forrest, *Inorg. Chem.* **2005**, *44*, 7992–8003; b) T. Sajoto, P. I. Djurovich, A. B. Tamayo, J. Oxgaard, A. A. Goddard III, M. E. Thompson, *J. Am. Chem. Soc.* **2009**, *131*, 9813–9822.

[14] R. J. Holmes, S. R. Forrest, T. Sajoto, A. Tamayo, P. I. Djurovich, M. E. Thompson, J. Brooks, Y.-J. Tung, B. W. D'Andrade, M. S. Weaver, R. C. Kwong, J. J. Brown, *Appl. Phys. Lett.* **2005**, *87*, 243507–1–243507–3.

[15] S. Haneder, E. D. Como, J. Feldmann, J. M. Lupton, C. Lennartz, P. Erk, E. Fuchs, O. Molt, I. Münster, C. Schildknecht, G. Wagenblast, *Adv. Mater.* **2008**, *20*, 3325–3330.

[16] a) C.-F. Chang, Y.-M. Cheng, Y. Chi, Y.-C. Chiu, C.-C. Liu, G.-H. Lee, P.-T. Chou, C.-C. Chen, C.-H. Chang, C.-C. Wu, *Angew. Chem. Int. Ed.* **2008**, *47*, 4542–4545; b) Y.-C. Chiu, J.-Y. Hung, Y. Chi, C.-C. Chen, C.-H. Chang, C.-C. Wu, Y.-M. Cheng, Y.-C. Yu, G.-H. Lee, P.-T. Chou, *Adv. Mater.* **2009**, *21*, 2221–2225.

[17] a) C.-H. Chien, S. Fujita, S. Yamato, T. Hara, T. Yamagata, M. Watanabe, K. Mashima, *Dalton Trans.* **2008**, 916–923; b) P. B. Hitchcock, M. F. Lappert, P. Terreros, *J. Organomet. Chem.* **1982**, *239*, C26–C30.

[18] L. Zhu, P. Guo, G. Li, J. Lau, R. Xie, J. You, *J. Org. Chem.* **2007**, *72*, 8535–8538.

[19] J. Li, P. I. Djurovich, B. D. Alleyne, M. Yousufuddin, N. N. Ho, J. C. Thomas, J. C. Peters, R. Bau, M. E. Thompson, *Inorg. Chem.* **2005**, *44*, 1713–1727.

[20] J. H. Jou, M.-F. Hsu, W.-B. Wang, C.-L. Chin, Y.-C. Chung, C.-T. Chen, J.-J. Shyue, S.-M. Shen, M.-H. Wu, W.-C. Chang, C.-P. Liu, S.-Z. Chen, H.-Y. Chen, *Chem. Mater.* **2009**, *21*, 2565–2567.

[21] K. Tsuchiya, E. Ito, S. Yagai, A. Kitamura, T. Karatsu, *Eur. J. Inorg. Chem.* **2009**, 2104–2109.

[22] T. Sajoto, P. I. Djurovich, A. B. Tamayo, J. Oxgaard, W. A. Goddard III, M. E. Thompson, *J. Am. Chem. Soc.* **2009**, *131*, 9813–9822.

[23] S.-J. Liu, Q. Zhao, Q.-L. Fan, W. Huang, *Eur. J. Inorg. Chem.* **2008**, 2177–2185.

[24] M. J. Frisch, G. W. Trucks, H. B. Schlegel, G. E. Scuseria, M. A. Robb, J. R. Cheeseman, J. A. Montgomery Jr., T. Vreven, K. N. Kudin, J. C. Burant, J. M. Millam, S. S. Iyengar, J. Tomasi,V. Barone, B. Mennucci, M. Cossi, G. Scalmani, N. Rega, G. A. Petersson, H. Nakatsuji, M. Hada, M. Ehara, K. Toyota, R. Fukuda, J. Hasegawa, M. Ishida, T. Nakajima, Y. Honda, O. Kitao, H. Nakai, M. Klene, X. Li, J. E. Knox, H. P. Hratchian, J. B. Cross, C. Adamo, J. Jaramillo, R. Gomperts, R. E. Stratmann, O. Yazyev, A. J. Austin, R. Cammi, C. Pomelli, J. W. Ochterski, P. Y. Ayala, K. Morokuma, G. A. Voth, P. Salvador, J. J. Dannenberg, V. G. Zakrzewski, S. Dapprich, A. D. Daniels, M. C. Strain, O. Farkas, D. K. Malick, A. D. Rabuck, K. Raghavachari, J. B. Foresman, J. V. Ortiz, Q. Cui, A. G. Baboul, S. Clifford, J. Cioslowski, B. B. Stefanov, G. Liu, A. Liashenko, P. Piskorz, I. Komaromi, R. L. Martin, D. J. Fox, T. Keith, M. A. Al-Laham, C. Y. Peng, A. Nanayakkara, M. Challacombe, P. M. W. Gill, B. Johnson, W. Chen, M. W. Wong, C. Gonzalez, J. A. Pople, *Gaussian 03*, Revision B.03, Gaussian, Inc., Pittsburgh, PA, **2003**.

Received: September 19, 2009
Published Online: January 19, 2010

 © 2010 Wiley-VCH Verlag GmbH & Co. KGaA, Weinheim